Lopez-Gordo et al. EURASIP Journal on Wireless Communications and Networking (2016) 2016:54
DOI 10.1186/s13638-016-0550-3

EURASIP Journal on Wireless Communications and Networking
a SpringerOpen Journal

RESEARCH Open Access

A proposal for bio-synchronized transmission of EEG/ERP data

M. A. Lopez-Gordo[1*], P. Padilla[1] and F. Pelayo Valle[2]

Abstract

Acquisition of event-related potentials (ERPs) requires a nearly perfect synchronization between the stimulus player and the EEG acquisition unit that clinical systems implement at hardware level by means of a wired link. Out of clinical context, current brain-computer interface technology offers wireless and wearable EEG headsets that provide ubiquitous EEG acquisition. However, they are not adequate for ERPs acquisition since they lack the physical wire with the stimulus player. In this paper, we propose a novel technique devoted to provide a solution to this problem by means of a bio-synchronization approach. This technique adds to the stimulus data, a tagged audio preamble for synchronization (TAP-S) that embeds a synchronization mechanism in its physiological response based on pseudo random sequences. In this way, the EEG data elicited by the preamble and the stimulus are recorded together and the stimulus onset can be directly extracted from the EEG data by preamble detection. TAP-S is tailored to work with any low-cost multimedia player and wireless EEG headsets. Our preliminary results reveal TAP-S as a first, promising, and low-cost approach that, after further improvement, could enable remote processing of ERPs with wireless acquisition with application in telemedicine, ambient assisted living, or brain-computer interfaces.

Keywords: Wireless EEG, Brain-computer interfaces, e-health, Telemedicine, Bio-synchronization

1 Introduction

EEG is a measure of the brain activity caused by populations of neurons that synchronously discharge their action potentials. An event-related potential (ERP) is the electrophysiological response evoked by an external stimulus that appears as positive or negative deflections of the EEG amplitude. In practical terms, ERPs are characterized by the amplitude and the latency with temporal reference to the stimulus onset. They are denoted by a letter P (positive) or N (negative) followed by a number that denotes the latency time in milliseconds since stimulus onset (e.g., P75, N100, and P200). ERP analysis is extensively used in clinical practice because their latencies and amplitudes correlate with well-known cognitive or physiological pathologies or functional impairments (e.g., long list with more than 20 visual abnormalities that includes optic neuropathy, multiple sclerosis, brain injury, and glaucoma [1, 2]). That means that an accurate estimation of the latencies and amplitudes is needed for diagnosis based on ERP analysis. The latter justifies the need of precise synchrony between the stimulus display and the EEG acquisition unit.

In clinical EEG systems, synchrony is typically implemented by means of a physical wire. Typically, the stimulation system is provided with a parallel port and specific software to run psycho-physiologic paradigms (e.g., e-Prime and Curry 7). In each trial, the software presents stimuli to the subject under test and immediately after sends onset marks out of a com port. These marks are received by the EEG acquisition unit though the hardware port (see Fig. 1). The onset mark is used to establish the beginning of the stimulus in a trial, thus setting the temporal reference to measure ERP latencies. The need of the wired link severely limits two fundamental aspects: (i) remote EEG/ERP acquisition and (ii) wireless EEG headsets. We elaborate on these two aspects in the next two paragraphs.

Telemonitoring is a key aspect for current e-health systems (see some current studies in [3–5]). Regarding remote EEG/ERP acquisition and testing, we merely mention some studies and cases of mobile and home-based EEG services. This service is gaining adepts

* Correspondence: malg@ugr.es
[1]Department of Signal Theory, Communications and Networking, University of Granada, Granada, Spain
Full list of author information is available at the end of the article

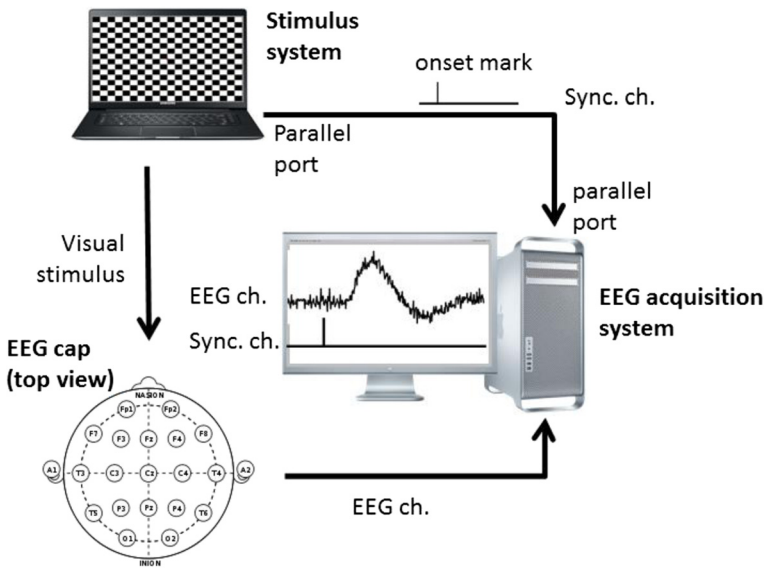

Fig. 1 Typical visual ERP acquisition setup composed of stimulus system and EEG acquisition system. Each time the stimulus system presents a stimulus, an onset mark is transmitted out from the parallel port to the EEG acquisition system. The onset mark demarcates the beginning of each trial

among clinicians and users. As a matter of fact, approximately 30 % of Dutch neurologists use EEG recordings for clinical diagnosis [6]. For instance, in [7], a telemedicine solution for remote video-EEG consultation was tried in La Rioja (Spain). Almost 99 % of patients expressed a high degree of satisfaction with the service. The authors of the paper concluded that users preferred the telemedicine service to in-hospital EEG test because it constitutes an improvement in access to this specialized medical care as well as important financial and time savings. The authors of [8] proposed a home-based polysomnography system as a cost-effective alternative for obstructive sleep apnea diagnosis. The system was equipped with a WiFi/3G interface for data and video communication via Skype. The authors of [6] compared the performance of four mobile EEG systems in recording epileptiform discharges. They concluded that most of the patients were satisfied with the service. There are more examples of home-based EEG [9–11] and medical services in general [12, 13]. However, these and other examples of home-based EEG and bio-signal testing do not apply to ERPs because of the nearly perfect synchrony needed between the stimulus player and EEG acquisition unit. Instead they register other long-term and non-related-to-events signals such as epileptic seizures or apnea episodes.

In respect to wireless EEG acquisition, we mention some studies and works related to brain-computer interfaces (BCIs) [14, 15]. In the last years, the technological evolution of BCIs has caused an increase of ambulatory, mobile, and wireless EEG headsets for clinic, entertainment, ambient assisted living, and other personal uses and applications [16–19]. The latest advance consists in low-cost, wearable and dry EEG headsets with wireless transmission (see [20, 21] for reviews) that allows mobile EEG services. These devices offer synchronization by means of proprietary software and protocols but not between the stimulus player and the wireless EEG headset. They are standalone solutions that do not integrate a stimulus player. Then, they are not meant to execute ERP paradigms but are suitable for others in which stimulation is not needed (e.g., self-regulation of low frequency cerebral rhythms [22], alpha band modulation [23] or steady-state EEG responses [24]). Conversely, other wireless EEG designs combine both stimulus player and EEG headset with synchronization [25, 26]. In [22], the latter attempt, specific clinical hardware for stimulation with a specific SYN port was used (PS33-PLUS, by Grass Technologies); although in terms of usability, we would expect wireless EEG headsets to permit users to use their own stimulus players without addition of extra synchronization hardware.

In summary, event-related paradigms are limited to clinical acquisition due to restrictions in synchrony. In this paper, we propose a technique, in the field of novel bio-inspired and bio-collaborative approaches [27, 28], aimed to address this limitation. Tagged audio preamble for synchronization (TAP-S) adds to the stimulation data a tagged audio preamble that embeds in its physiological response a synchronization mechanism based on pseudo random sequences. Our preliminary results reveal TAP-S as the first, promising, and low-cost approach that could enable recordings of ERPs with wireless EEG headsets and remote processing with application in

telemedicine, ambient assisted living, or brain-computer interfaces.

2 TAP-S overview

2.1 The synchronization issue in ERP acquisition

In medical diagnosis, ERP estimation is typically performed by synchronous trials averaging. Paradigms normally average tens or hundreds of trials to obtain high quality ERPs (e.g., a minimum of 64 and 128 are recommend for visual evoked potentials [29]). Conversely, if the stimulus onset could not be accurately determined (asynchronous averaging), this would give rise to inaccurate latencies and lower amplitudes. Figure 2 illustrates this effect.

2.2 Applications

The main idea behind TAP-S is to provide an accurate synchronization mechanism between the stimulus player and wireless EEG headset without the need of a physical wire. This is a key aspect to develop innovative mobile EEG services. We just mention some examples in what follows.

- Interactive services: Fig. 3 shows messages flow in a mobile EEG service. In the scenario of Fig. 3, the stimulation server stores the stimulus content. In an online application, it streams both a preamble and stimulation down to the stimulation player. The stimulation player buffers or reproduces it online, thus evoking the corresponding brain response on the user. A wireless EEG headset acquires this brain response and uploads the EEG data to the monitoring and processing server. In an online application, this server analyzes the brain response and immediately takes a decision. This decision modifies the next stimulation to be streamed down to the subject, thus closing the interactive loop.

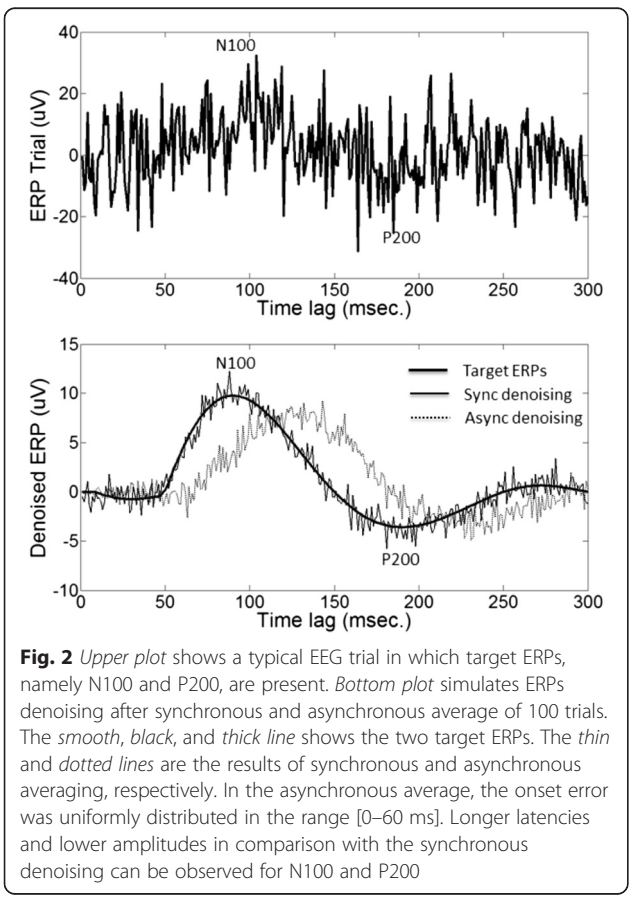

Fig. 2 *Upper plot* shows a typical EEG trial in which target ERPs, namely N100 and P200, are present. *Bottom plot* simulates ERPs denoising after synchronous and asynchronous average of 100 trials. The *smooth*, *black*, and *thick line* shows the two target ERPs. The *thin* and *dotted lines* are the results of synchronous and asynchronous averaging, respectively. In the asynchronous average, the onset error was uniformly distributed in the range [0–60 ms]. Longer latencies and lower amplitudes in comparison with the synchronous denoising can be observed for N100 and P200

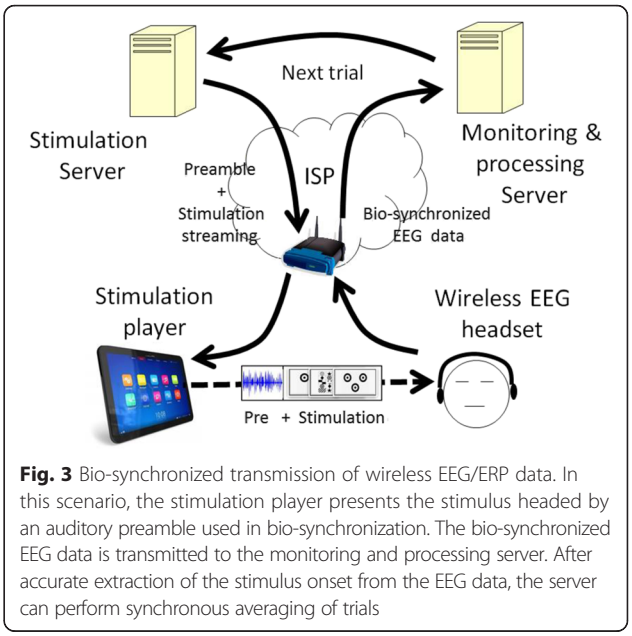

Fig. 3 Bio-synchronized transmission of wireless EEG/ERP data. In this scenario, the stimulation player presents the stimulus headed by an auditory preamble used in bio-synchronization. The bio-synchronized EEG data is transmitted to the monitoring and processing server. After accurate extraction of the stimulus onset from the EEG data, the server can perform synchronous averaging of trials

This type of interactive service could permit online cognitive telerehabilitation, such as neuro-feedback applied to a multitude of pathologies (e.g., attention deficit hyperactivity disorder [30, 31], autism spectrum [32, 33], cerebral palsy [34], and mental impairment [35]).

Notice that IP protocols offer synchronization mechanisms in all links and interfaces of Fig. 3 except in the interface between the stimulation player and the wireless EEG headset. In this link, TAP-S provides it.

- Ubiquitous execution of event-related paradigms: since the synchronization provided by TAP-S is embedded in the EEG data, both the online and the offline execution of event-related paradigms could be performed. As an example, Fig. 4 shows a scenario of use: a volunteer (for instance a female) in a clinical study of vision downloads her video. It is stored in her mobile devices or her stimulus player. Then, during the commuting, she plays it. The wireless EEG headset acquires the brain responses and stores the EEG data. Then, it uploads them

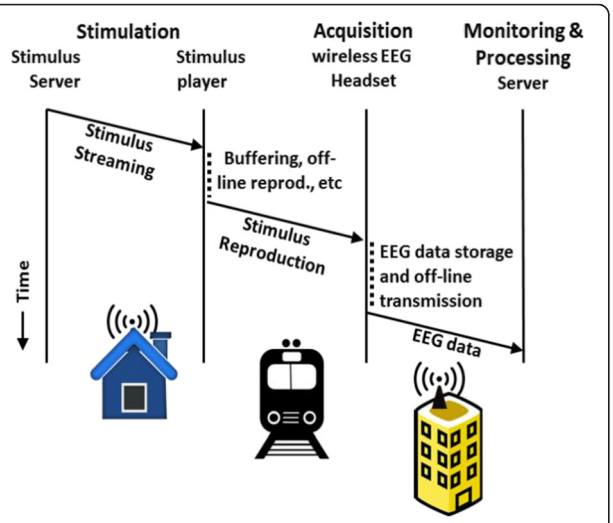

Fig. 4 Ubiquitous execution of event-related paradigms. In this scenario, participants in a study of vision assessment download a video at home and store it in their mobile devices. Then, during their daily commuting, they play it. The wireless EEG headsets store the EEG data and transmit them to the monitoring and processing server at work. This server detects the stimulus onset of each trial by means of TAP-S and performs asynchronous averaging of ERPs

to a remote monitoring and processing server when a broadband connection is available (for instance at office). This server detects the stimulus onset of each trial by means of TAP-S and performs ERP analysis.

2.3 Design

TAP-S is implemented by encapsulating the stimulation data with a synchronization preamble (see Fig. 5).

2.3.1 Physical principles

TAP-S is based on the reliable evocation of auditory middle-latency responses, precisely the well-known 40-Hz phenomenon [36, 37]. We explain it as follows.

Tone-pips are commonly used in clinical audiology [38, 39]. They are auditory pulses containing pure tones of few milliseconds duration with rising and falling flanks. When we stimulate someone with a single auditory tone-pip, it evokes potentials that resemble 3 or 4 cycles of a 40-Hz sine wave. Consequently, when a train of auditory clicks is presented at a rate of 40 stimuli per second, these waves combine to form a sinusoidal wave of 40 Hz (see Fig. 6). There are two important reasons that justify the use of the 40-Hz ERP: (i) this potential is a reliable and time-locked response to the stimulus onset; (ii) the energy is concentrated around the 40 Hz spectral line (i.e., most of the power spectral density is within a very short spectral range). These two aspects are very important for a robust and reliable detection.

2.3.2 Preamble design

In specialized literature, middle-latency auditory potentials, such as the 40-Hz phenomenon [40–42], have been evoked by means of tone-pips. Equation 1 shows an analytic expression of a tone-pip.

$$g(t) = \begin{cases} {}^{t}/_{t_1} \sin(2\pi f_c t) & 0 \le t \le t_1 \\ \sin(2\pi f_c t) & t_1 \le t < t_2 \\ {}^{(t-t_3)}/_{(t_2-t_3)} \sin(2\pi f_c t) & t_2 \le t \le t_3 \end{cases} \quad (1)$$

where $g(t)$ is the tone-pip signal, t_1 and t_2 delimit the rising and falling times, f_c is the pure tone frequency, and t_3 is the total length (see Section 3 for specific values used in this study).

We also obtained $m(t)$, which is a pseudo random binary sequence of maximum-length (MLS or m-seq) presented at a rate of 40 Hz (i.e., 25 ms time interval) (2)

$$m(t) = \sum_{m=0}^{M-1} a_m \delta(t - 0.025m) \quad (2)$$

where a_m is the m-seq and M is the length of the sequence. Pseudo random codes have been extensively used for synchronization purposes in navigation/positioning [43, 44], radar [45], and wireless communications [46, 47] and for other purposes related to clinical practice ([48–50]), etc. In the case of m-seq, its autocorrelation function cannot be bettered by any other family of pseudo random codes.

Finally, we convolved $g(t)$ and $m(t)$ (3), thus giving rise to an auditory signal designed to evoke the auditory 40-

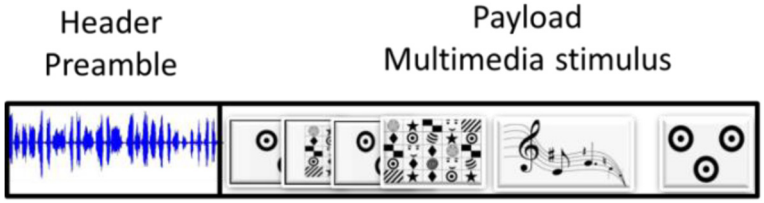

Fig. 5 TAP-S encapsulates the multi-modal stimulus data with a header containing the auditory synchronization preamble

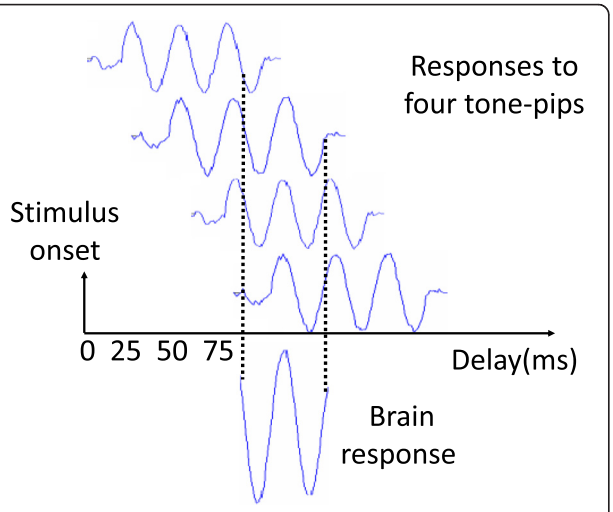

Fig. 6 The auditory 40-Hz phenomenon. The figure shows four auditory middle-latency responses to four tone-pips presented at a rate of 40 Hz (25 ms time interval). On the *bottom*, the overlapped response represents the coherent sum (i.e., in phase) of the four responses. The figure is adapted from [36]

Hz phenomenon at the same time that permits an accurate detection based on its autocorrelation properties

$$p_{40\text{hz}}(t) = m(t) \otimes g(t) \tag{3}$$

where $p_{40\text{hz}}(t)$ is the signal used as synchronization preamble.

2.3.3 Preamble detection

We detect the preamble by means of a replica-correlator detector (equivalent to a matched filter detector [45]). There are two ways to build the replica signal, either by averaging many ERPs during a previous calibration session or synthetically by software. In this study, we decided the second option, thus avoiding calibration sessions and challenging the study under a plug-and-play approach. The replica signal was the expected electrophysiological response to the stimulus signal $p_{40\text{hz}}(t)$ and was synthetically built as the convolution of the $m(t)$ with 3 cycles of a 40-Hz sinusoidal signal. We used receiver operating characteristic (ROC) curves [51] and area under the curve (AUC) to assess the discrimination capacity of TAP-S. In addition, we estimated the best operating point (BOP).

2.3.4 Encapsulation process

The encapsulation and decapsulation processes occur at the stimulation and the monitoring and processing servers, respectively (see Fig. 7). The processes are completely transparent for the stimulus player and the wireless EEG headset. The stimulus player reproduces the whole message (preamble and stimulation data), and the preamble evokes the auditory 40-Hz phenomenon. Then, the wireless EEG headset uploads to the monitoring and processing server EEG data containing the brain responses to both preamble and stimulus. The monitoring and processing server detects the synchronization preamble and removes it from the EEG data, thus obtaining the stimulus response. The only thing that the monitoring and processing server needs to perform for the detection of the preamble is to build the replica signal (see previous subsection). In turn, the replica signal is built with only three parameters of the pseudo random sequence: (i) number of taps, (ii) cyclical shift, and (iii) initiation seed.

2.4 Operation restrictions

TAP-S has only one restriction for an optimal synchronization. The media player must reproduce the stimulus data stream, including the preamble, in continuous mode. Buffering or playback is permitted, as well as online or offline upload of the EEG data. The only restriction is that both preamble and stimulus must be reproduced together without gaps, that is, without

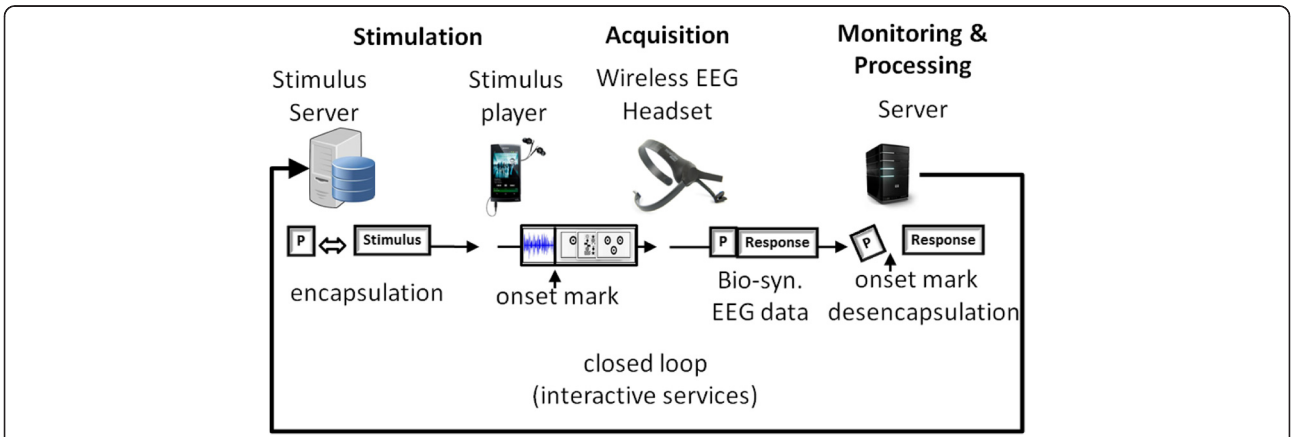

Fig. 7 The encapsulation process. Encapsulation and decapsulation only happens at both ends, that is, in the stimulation and the monitoring and processing servers. It is transparent for both the stimulus player and wireless EEG headset

interruptions once the stimulation is started. Uninterrupted reproduction is mandatory because the synchronization process requires a replica signal that matches the response to the signal $p_{40\text{hz}}(t)$.

3 Methods

In this preliminary study, we pursue (i) the assessment of preliminary results of TAP-S as the first bionic synchronization mechanism of data transmission and (ii) the analysis of its practical utility in medical diagnosis. In this experiment, we used a clinical EEG system in an isolated lab with a wired link between the stimulation and the acquisition units (similar to Fig. 1). The onset marks obtained with this configuration was considered the gold standard. Then, we tried the blind detection of the onset marks by means of TAP-S.

3.1 Experimental procedure

Two healthy volunteers participated (both males, 31 and 41 years old). The experiment was undertaken in a room isolated from external disturbances. The study was meant to be completely auditory, so blind volunteers could participate if necessary (see [52] for a discussion about the controversy in auditory vs. visual BCIs). Then, participants were told to close their eyes during the whole experiment, thus facilitating concentration and avoiding muscular EEG artifacts (e.g., eyes blinking or involuntary gazing). The auditory stimulation was manually adjusted to the comfort level of each participant. They were informed of all aspects of the study and signed the informed consent.

The experiment consisted of 21 trials with the same structure. First, an allocution indicated trial start after key pressing. Once the participant pressed a key, a beep announced the beginning of the trial. After the beep, the preamble was presented to the participant by means of earphones. Finally, a beep sounded and an allocution signaled the end of the trial and the preparation for the next one. The duration of each trial was around 6 s, and the inter-trial resting time was up to the participant (typically 15–25 s). The goal was to avoid cumulative effects along the trials (e.g., fatigue and lack of focus on the experiment).

3.1.1 Recording

For the sake of usability, we configured a single active channel placed on the vertex (Cz) and referenced to the mean value of the ear lobes (see Fig. 8). These positions of the International 10-20 system [53] were chosen because they have been included in reports of successful studies of auditory event-related potentials [54–57] and because various commercial wireless EEG headsets have an electrode on or close to this position. The ground electrode was placed between the Fpz and the Fz positions. The recordings were acquired on a Synamps2 by Compumedics Neuroscan, were band-pass filtered between 1 and 100 Hz, and were sampled at a rate of 1 kHz.

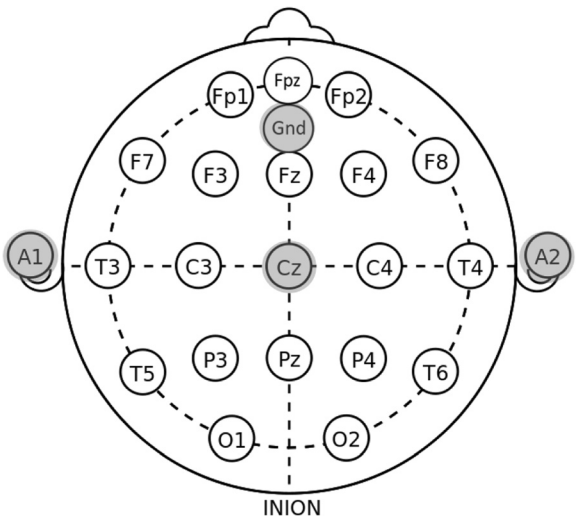

Fig. 8 *Top view* of the International 10-20 system for electrode placement. The positions of electrodes used in this study have a *gray* background

3.1.2 Preamble header

The preamble was built by means of an m-seq of 8 taps (length = $2^8 - 1 = 255$). We constructed $m(t)$ by spacing out 25 ms each of the symbols of the m-seq. Then, $m(t)$ was convolved with a tone-pip as described in (1) with f_c equals 1 kHz and t_1, t_2, and t_3 equal 1, 4, and 5 ms, respectively, thus obtaining $p_{40\text{hz}}(t)$, which constitutes the preamble header (see Fig. 9). The total length of the header was 6.375 s. The values used in this experiment are the typical ones used in specialized literature [38, 39]. Preambles were generated using the same m-seq.

3.1.3 Detection

We generated a synthetic replica of the expected EEG response to the preamble. This signal was built by convolution of $m(t)$ with 3 cycles of a 40-Hz sinusoidal signal. The preamble was detected by means of the replica-correlator detector with inputs from the recorded EEG signal and the replica. The output of the replica-corrector was either detection of a preamble (true positive or TP) or detection of an artifact (false positive or FP). We varied the detection threshold to estimate the ROC. The BOP was chosen as the detection threshold that maximized (4)

$$10log_{10}\left[(\text{TP})^2/(\text{TP}+\text{FP})\right] \tag{4}$$

where (TP + FP) is the total number of detections and TP is the number of detected preambles. In the case of trial averaging with perfect synchronous averaging, FP

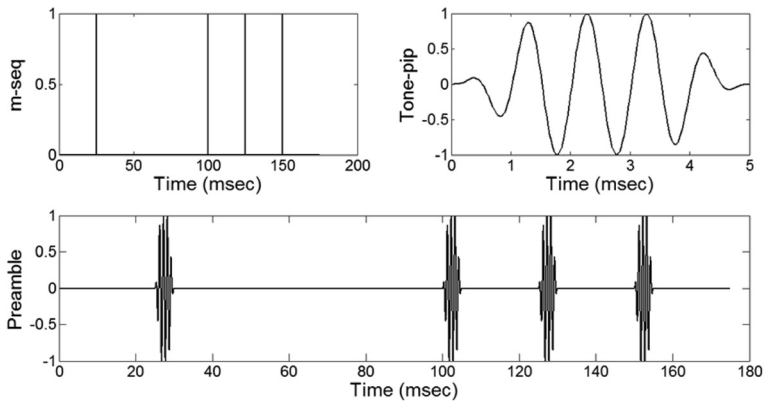

Fig. 9 Generation of the preamble header. The *upper part* of this figure shows the two signals involved in the generation of the preamble, namely the m-seq (*upper left plot*) and the tone-pip (*upper-right plot*). In this illustrative example, we present a fragment of an m-seq with codes [0 1 0 0 1 1 1]. The tone-pip is generated as a 1-kHz tone of 5-ms duration with rising and falling flanks of 1 ms each. On the *bottom*, the plot shows the convolution of both

equals zero and TP equals the number of trials. Then, (4) would yield the maximum denoising capacity in terms of SNR. In addition, we computed the AUC, which represents the ability of TAP-S to detect preambles correctly.

Some simple rules were adopted to reduce the number of FPs. We excluded the beginning and the end of the EEG signals to avoid electrical artifacts due to electrode impedance measurement, initial calibration of amplifiers, filters setting, etc. The replica-correlator detector found peaks that exceeded the threshold with a minimum separation guard between them. If two peaks were detected within the separation guard, then the one with the highest amplitude was considered as preamble detection. If the separation between peaks was longer than the separation guard, then both were considered two independent detections. The upper limit of the separation guard is the duration of the preamble, namely 6.375 s, because this is minimum time between two consecutive trials without resting time. The minimum separation time is twice the length of a pulse of 3 cycles of the 40-Hz phenomenon, namely 150 ms, because it is the width of its autocorrelation function.

With these two limits, we did some preliminary trials and we estimated that a time guard of 2 s was a flexible choice that keeps balance between a low rate of false positives and a good time resolution for peak scrutiny.

3.1.4 EEG signal preprocessing

To suppress artifacts (e.g., due to muscular movement or induced by electrical glitches), any EEG amplitudes larger than 50 μV were grounded before presented to the replica-correlator detector.

The output of the replica-correlator in the absence of noise is a pass-band signal (a *sinc* function centered at 40 Hz). Since we preferred a base-band signal to perform detection of peaks of synchrony, we used a simple envelope detector (half-wave rectifier and low-pass filter) to obtain the base-band signal. The width of the main lobe of the *sinc* function in the frequency domain is the inverse of the duration of the 40-Hz phenomenon, that is, 3 cycles of 40 Hz. Then, the total length corresponds to 75 ms and the inverse is 13.3 Hz. This was the 3-dB cutoff frequency of the low-pass filter. The filter consisted in a second order Butterworth filter that was executed forward and reverse to cancel phase shifts. Note that the net effect is a fourth order filter with 6 dB of loss at the original 3 dB cutoff frequency.

The filtering process explained in this section is applied to the whole EEG acquisition, and the main goal is the detection of the preamble. In a clinical application, the specific processing of trials is typically specified by the clinical protocol.

4 Results

The plots and tables of this section are intended to reveal the main goals of this experiment, namely the assessment of preliminary results of TAP-S as bio-synchronization mechanism (Figs. 10 and 11 and Table 1) and the analysis of its practical utility in medical diagnosis (Table 2 and Fig. 12).

Figure 10 contains relevant information about the detection performed at the BOP for subjects 1 and 2. It shows the output of the replica-correlator detector, the onset marks provided by the clinical EEG system, the onset marks detected by TAP-S, and the best detection threshold corresponding to the BOP (dotted horizontal line).

Figure 11 shows the ROC curves for both subjects. The AUC was $AUC_1 = 0.99$ and $AUC_2 = 0.70$ for subjects 1 and 2, respectively. The BOP was considered the detection threshold that maximized (4). These maximum values for each subject, in dB units, were $BOP_1 = 12.6$ dB

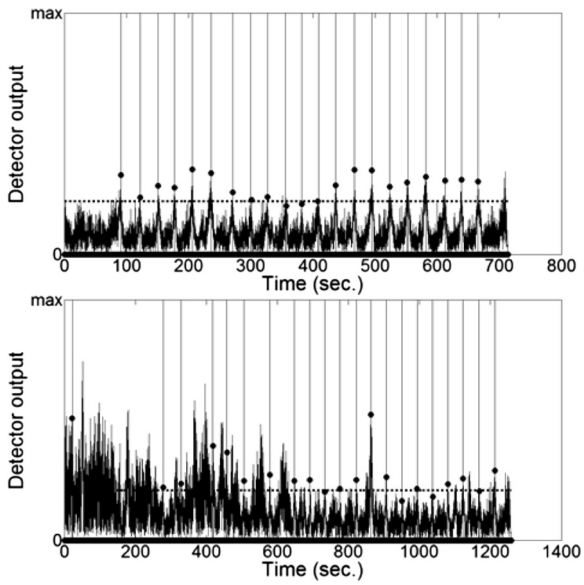

Fig. 10 TAP-S performance at BOP for subjects 1 and 2 (*upper* and *bottom plots*, respectively). It shows the output of the replica-correlator detector (the *noisy background*), the onset marks provided by the clinical EEG system (the *vertical lines*), the onset marks detected by TAP-S (the *filled circles*), and the best detection threshold corresponding to the BOP (the *dotted horizontal line*). In the *X*-axis, the length of the experiment in seconds. In the *Y*-axis, the output of the detector in arbitrary units

and $BOP_2 = 7.7$ dB (see Table 1). Assuming perfect synchrony, these values correspond to the maximum improvement in SNR of ERPs after trial averaging with respect to a single trial.

Table 1 shows statistics of the detection at the BOP, namely the TF, FP, accuracy, and confidence intervals of a proportion at a significance level $\alpha = 0.05$.

Table 2 shows details about the synchrony for the 21 trials in both subjects. The first column of each subject indicates the absolute time of each trial onset referenced

Table 1 Statistic at BOP

Subject 1	Subject 2
TP 20	TP 19
FP 1	FP 43
acc 0.95	acc 0.31
Uppb 0.99	Uppb 0.21
LowB 0.77	LowB 0.43
maxG (dB) 12.6	maxG (dB) 7.7

to the beginning of the experiment. For instance, the first trial of subject 1 initiated 90.765 s after the experiment started. This first column (real) represents the gold pattern. The second column (TAP-S) indicates the onset time yielded by TAP-S. The last column (err.) computes the difference between the first and second columns, that is, the error in synchrony. Italics indicate trials for which TAP-S was unable to detect a valid preamble. This is the case when the error was longer than 150 ms. They were considered as outliers and not taken into account for the calculation of mean and standard deviation (see bottom rows of Table 2).

Based on the results of Table 2, the example of Fig. 12 illustrates the effects of trial averaging after using TAP-S and with perfect synchrony. For this purpose, synthetic ERPs, namely N100 and P200, were generated and used as patterns (thin lines in the snapshots). The two main plots of Fig. 12 show for subjects 1 and 2 (upper and bottom plots, respectively) the TAP-S-based trial averaging of the synthetic ERPs, assuming as synchrony errors as shown from the values of Table 2 (thick lines). Also, they show perfectly synchronous trial averaging (thin lines). The small snapshots on the upper-right corners correspond to a zoom-in of the central part of each main plot. The errors in synchrony with respect to the N100 and P200 components were less than 1 ms and −11 ms for subjects 1 and 2, respectively. See

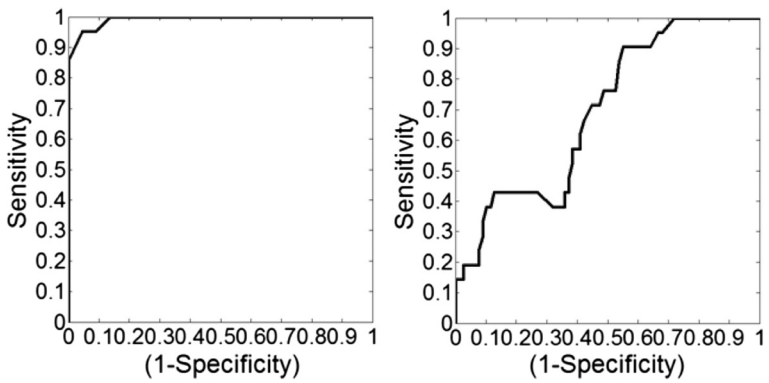

Fig. 11 ROC curves for subjects 1 and 2 (*left* and *right plots*, respectively)

Table 2 Stimulus onset (seconds)

#Trial	Subject 1			Subject 2		
	real	TAP-S	err.	real	TAP-S	err.
1	90.765	90.772	0.007	23.675	21.640	*−2.035*
2	121.749	121.757	0.008	278.444	278.428	−0.016
3	150.968	150.950	−0.018	329.208	329.159	−0.049
4	177.318	177.307	−0.011	418.073	418.502	*0.429*
5	205.917	205.918	0.001	457.121	458.596	*1.475*
6	236.420	236.414	−0.006	505.796	505.562	*−0.234*
7	270.897	270.913	0.016	578.665	578.662	−0.003
8	299.546	301.379	*1.833*	647.968	647.973	0.005
9	326.715	326.744	0.029	691.898	691.807	*−0.091*
10	355.814	357.070	*1.256*	733.787	733.820	0.033
11	382.487	382.496	0.009	776.155	776.165	0.010
12	409.485	407.748	*−1.737*	822.684	822.685	0.001
13	436.793	436.782	−0.011	863.685	863.679	−0.006
14	467.164	467.150	−0.014	906.591	906.580	−0.011
15	494.971	494.968	−0.003	950.752	950.725	−0.027
16	523.333	523.319	−0.014	993.821	992.964	*−0.857*
17	553.099	551.617	*−1.482*	1036.838	1037.803	*0.965*
18	582.205	582.192	−0.013	1080.809	1080.939	0.130
19	612.743	612.743	0.000	1123.278	1123.241	−0.037
20	639.022	639.033	0.011	1168.036	1169.512	*1.476*
21	666.127	666.117	−0.010	1212.946	1212.918	−0.028
Mean			−0.001			−0.017
Std			0.013			0.031

Section 5.2 for discussion regarding the impact of these error magnitudes.

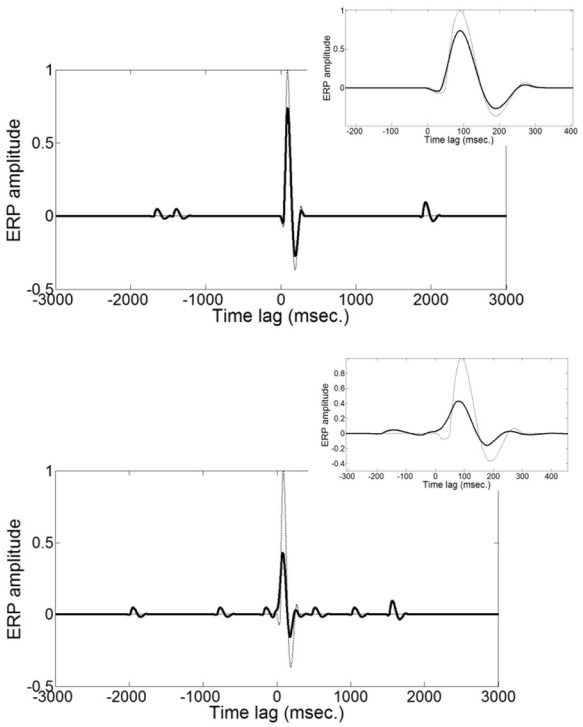

Fig. 12 Illustrative example with TAP-S. *Thin lines* in the snapshots show target ERPs (N100 and P200) used as patterns for trial averaging. The two main plots show for subjects 1 and 2 (*upper* and *bottom plots*, respectively) the TAP-S-based trial averaging of the target ERPs taken as the error of synchrony as shown from the values of Table 2 (*thick lines*). Also, they show synchronous trial averaging (*thin lines*). The small snapshots on the *upper* corners correspond to a zoom-in of the central part of each main plot. In the case of the TAP-S, no relevant deformation can be observed from the shape of ERPs, and in the case of subject 1, a negligible delay with respect to the synchronous trial averaging. In the *X*-axis, time in milliseconds. In the *Y*-axis, amplitude of ERPs in arbitrary units

5 Discussion

In this section, we discuss the results in terms of detection performance and medical diagnosis utility. In summary, our preliminary results with two subjects support that TAP-S is capable to provide bio-synchronization by means of the 40-Hz response. However, the dissimilar results between subject 1 and subject 2 suggest that additional testing is required before TAP-S could be considered efficient enough for clinical applications.

5.1 Performance of TAP-S

Figure 10 shows detection performance at BOP for both subjects. The bottom plot shows a much more noisy aspect than the upper plot. We analyzed the EEG raw signals from both subjects, and the ones corresponding to subject 2 presented many more EEG artifacts. It could be due to muscular movements or nervous behavior during the trials (in fact, this subject recognized that this was his very first experience in this type of experiments). In some technologies such BCIs, it is assumed that they do not work for everyone [58] (i.e., BCI illiteracy). It could be stated that even though BCIs do not work for everyone, evoked potential recording does. That is, auditory potentials evoked by the recommended protocol (clinical instrumentation, setup, number of electrodes and positions, stimuli intensity, number of averages, signal preprocessing, etc.) are reproducible. Our proposal does not follow any clinical protocol since we pursued a simple plug-and-play approach (e.g., only one active electrode, no calibration session, and the use in detection of a generic replica) suitable for future plug-and-play BCI applications. Another justification for the poor performance of subject 2 could be in the stimulus used for the evocation of the 40-Hz response. Under our plug-and-play approach, the design of the stimulus was the same for both subjects. However, many aspects influence the amplitude of the 40-Hz response and, hence, the SNR of the signal to be detected (e.g., the intensity and auditory threshold of each person or the optimal

carrier of the tone-pip). In addition, it has been reported that the optimal peaking frequency of the 40-Hz response probably varies (in the range 35–45 Hz) from one person to the next [36]. The latter would lead to variances of the amplitude of the 40-Hz response that could justify the differences in performance between subjects 1 and 2. For sure, a calibration session would have improved the results of both subjects, but at the cost of our plug-and-play approach. Under these circumstances, entire success cannot be expected. This is the cost of the human factor. However, and despite the noisy aspect of the bottom plot, TAP-S was able to filter most of them due to the time guard defined in the methodological section (at BOP, only FP = 43 and TP = 19). It is important to consider that for a high rate in successful detection, some premises were introduced in the detection, namely the initial and end periods and the time guard. Without this information, the number of FPs would have increased. It is important to understand that this prior information only filters out FPs in the scale of seconds (e.g., separation guard was 6.375 s). This is not relevant to TAP-S and does not affect the essence of this experiment because TAP-S concerns synchronization in the millisecond scale. Synchronization in the scale of seconds between the media player and the EEG headset can be easily performed by IP protocols or even manually.

Figure 11 shows the ROC curves for both subjects. A rough guide for classifying the accuracy of a test based on the AUC is the traditional academic point system [59]: 1.0 perfect; 0.90–0.99 excellent; 0.80–0.89 good; 0.70–0.79 fair; 0.60–0.69 poor; 0.50–0.60 worthless. In our study, the detection of preamble was excellent ($AUC_1 = 0.99$) and fair ($AUC_2 = 0.70$) for subjects 1 and 2, respectively. Then, the performance of TAP-S as preamble detector can be considered as excellent and fair for subjects 1 and 2, respectively.

Table 1 shows some details about the detection performance at the BOP. The large difference in accuracy between subject 1 (acc1 = 0.95) and subject 2 (acc2 = 0.31) is justified by the noise at the output of the replica-correlator detector (Fig. 8, bottom). The maximum improvement of SNR after trial averaging is remarkable (see Table 1, last row). It must be interpreted as the denoising capacity of TAP-S in this study. The maximum theoretical capacity, considering 0 FPs and 21 TPs is 13.2 dB by direct application of (4). Then, subject 1 achieved almost the maximum (12.6 dB).

We finalize this section mentioning that the scope of this experiment was not to obtain the highest performance in detection but to show evidence that synchronization in the range of milliseconds can be performed with TAP-S. As stated before, EEG is considered a non-stationary signal with large variations in inter-trials for the same subject and inter-subjects. The ROC curve showed a completely satisfactory performance for one subject. Consequently, it is more than enough to think of TAP-S as a promising technique that deserves to be optimized in future works.

5.2 Usefulness of TAP-S in medical diagnosis

Table 2 shows the numerical results on the detection of the onset marks. An aspect that deserves to be discussed is the large error values in the table (italics). It is obvious that the TAP-S did not work in all trials and some outliers happened. However, the gist of the discussion should orbit around the applicability of TAP-S in medical diagnosis with wireless EEG headset. The question to address are the following: (i) What would happen if some of the trials were detected with large synchronization errors? The immediate answer is that the corresponding EEG data would contain nothing but uncorrelated EEG that do not disturb the detection, except that more number of trials are needed to achieve a certain target SNR; (ii) What would be the effect of small errors around 20–50 ms? Small errors would give rise to a smoother shape but they would have no effect on the latency since negative and positive errors would cancel each other after a sufficient number of averages. Furthermore, results of subject 1 (see Table 2) show a very low number of errors in this time window (only 1 out of the 21 trials). The low number of small errors is justified because FPs are distributed in a large time window (from few milliseconds to seconds) and not only in the 20–50-ms window. Therefore, we expect a relative small number of small errors, thus having a minor impact on the shape. The next question would be, How would it affect the quality of the registered ERPs? In clinical practice, ERPs are estimated by averaging a high number of trials. Averaging of some trials with uncorrelated EEG data would just decrease the SNR of the ERPs, but the latencies and shape of the averaged ERPs would remain unaltered. It is interesting to point out that FPs with errors of several hundreds of milliseconds affect less than those with few milliseconds because the latter contain partial correlated EEG data. Figure 12 is an illustrative example of this with results reported in Table 2. Italics of the table are easily identified because, after trial averaging, they become small and positioned far from the zero lag. The snapshot of subject 1, at the upper-right corner of the main plot, shows with detail that the averaged trials yield N100 and P200 peaks with near zero error in latency with respect to the synthetized ERP. Furthermore, the envelope remains almost the same. This justifies the usability of TAP-S in medical diagnosis with wireless EEG teleservices.

6 Conclusions

In this paper, we propose a novel technique that provides synchronization for wireless EEG acquisition. TAP-S adds a preamble to the stimulation data that embeds in its

neuro-physiological response a synchronization mechanism based on pseudo random sequences.

Despite a promising performance, still many open questions remain. For instance, the impulse response was assumed to be 3 cycles of 40 Hz. It could be optimized by individual basis with a previous calibration session. Also, the type of potential used for the preamble (the mid-latency auditory 40 Hz) could be substituted by others. Nothing prevents the use of visual stimulus instead of auditory. In fact, there are some pioneering studies about time-locking visual stimulus [60, 61]. Another fact is the design of the preamble. A sequence of 255 seemed to be a good trade-off between the detection performance and the overhead added to the stimulus. In our study, this overhead was just 6.375 s, while the recommendation to obtain visual ERPs is longer than 30 s (more than one sweep, each sweep containing 64 stimuli at a rate of two stimuli per second [29]). Furthermore, the stimulus data could be encapsulated by a header and tail, both for synchronization purposes, thus augmenting detection performance at the cost of overhead increasing.

To the best of our knowledge, this is the first attempt to provide a synchronization mechanism based on brain signals used in wireless ERP acquisition. Our very first design remarkably worked with one subject. This is the most relevant contribution of this work and it proves that TAP-S is a feasible approach that deserves to be improved. After further improvements, the level of synchronization provided by TAP-S would let remote assessment of ERPs and online analysis, thus opening the door to interactive mobile EEG applications.

Competing interests
The authors declare that they have no competing interests.

Acknowledgements
This work was supported and co-financed by Nicolo Association for the R&D in Neurotechnologies for disability, the research project P11-TIC-7983, Junta of Andalucia (Spain), the Spanish National Grant TIN2015-67020, co-financed by the European Regional Development Fund (ERDF) and the CASIP research group TIC-117. We thank the Bio-engineering Institute of the University of Miguel Hernández of Elche (Spain), where part of this study was undertaken as a research stay.

Author details
[1]Department of Signal Theory, Communications and Networking, University of Granada, Granada, Spain. [2]Department of Architecture and Computers Technology, University of Granada, Granada, Spain.

Received: 20 October 2015 Accepted: 4 February 2016
Published online: 19 February 2016

References
1. MA Ahluwalia, SD Vold, Visual evoked potentials and glaucoma. Glaucoma Today. 39–40 (2014). http://glaucomatoday.com/2014/10/.
2. A. Van Den Bruel, J. Gailly, F. Hulstaert, S. Devriese, M. Eyssen, The value of EEG and evoked potentials in clinical practice KCE reports 109C, (2009)
3. S Tennina, M Di Renzo, E Kartsakli, F Graziosi, AS Lalos, A Antonopoulos, PV Mekikis, L Alonso, WSN4QoL: a WSN-oriented healthcare system architecture. Int. J. Distrib. Sens. Netw. **2014**, 1–16 (2014)
4. E Kartsakli, A Antonopoulos, A Lalos, S Tennina, M Renzo, L Alonso, C Verikoukis, Reliable MAC design for ambient assisted living: moving the coordination to the cloud. IEEE Commun. Mag. **53**, 78–86 (2015)
5. E Kartsakli, A Lalos, A Antonopoulos, S Tennina, M Renzo, L Alonso, C Verikoukis, A survey on M2M systems for mHealth: a wireless communications perspective. Sensors. **14**, 18009–18052 (2014)
6. J Askamp, MJAM van Putten, Mobile EEG in epilepsy. Int. J. Psychophysiol. **91**, 30–35 (2014)
7. C Campos, E Caudevilla, A Alesanco, N Lasierra, O Martinez, J Fernández, J García, Setting up a telemedicine service for remote real-time video-EEG consultation in La Rioja (Spain). Int. J. Med. Inf. **81**, 404–414 (2012)
8. M Bruyneel, S Van den Broecke, W Libert, V Ninane, Real-time attended home-polysomnography with telematic data transmission. Int. J. Med. Inf. **82**, 696–701 (2013)
9. F Brunnhuber, D Amin, Y Nguyen, S Goyal, MP Richardson, Development, evaluation and implementation of video-EEG telemetry at home. Seizure. **23**, 338–343 (2014)
10. E Goodwin, RH Kandler, JJP Alix, The value of home video with ambulatory EEG: a prospective service review. Seizure. **23**, 480–482 (2014)
11. JJP Alix, RH Kandler, SR Mordekar, The value of long term EEG monitoring in children: a comparison of ambulatory EEG and video telemetry. Seizure. **23**, 662–665 (2014)
12. N Patwari, J Wilson, S Ananthanarayanan, SK Kasera, DR Westenskow, Monitoring breathing via signal strength in wireless networks. IEEE Trans. Mob. Comput. **13**, 1774–1786 (2014)
13. L Guo, C Zhang, J Sun, Y Fang, A privacy-preserving attribute-based authentication system for mobile health networks. IEEE Trans. Mob. Comput. **13**, 1927–1941 (2014)
14. N Birbaumer, N Ghanayim, T Hinterberger, I Iversen, B Kotchoubey, A Kübler, J Perelmouter, E Taub, H Flor, A spelling device for the paralysed. Nature. **398**, 297–298 (1999)
15. MA Lopez-Gordo, F Pelayo, A binary phase-shift keying receiver for the detection of attention to human speech. Int. J. Neural Syst **23**(4), 130418190845004 (2013)
16. A Nijholt, DP-O Bos, B Reuderink, Turning shortcomings into challenges: brain–computer interfaces for games. Entertain. Comput. **1**, 85–94 (2009)
17. L-D Liao, C-Y Chen, I-J Wang, S-F Chen, S-Y Li, B-W Chen, J-Y Chang, C-T Lin, Gaming control using a wearable and wireless EEG-based brain-computer interface device with novel dry foam-based sensors. J. NeuroEngineering Rehabil. **9**, 5 (2012)
18. P Chang, KS Hashemi, MC Walker, A novel telemetry system for recording EEG in small animals. J. Neurosci. Methods. **201**, 106–115 (2011)
19. R Matthews, PJ Turner, NJ McDonald, K Ermolaev, TM Manus, RA Shelby, M Steindorf (2008). Real time workload classification from an ambulatory wireless EEG system using hybrid EEG electrodes. (30th Annual International IEEE EMBS Conference Vancouver, British Columbia, Canada, 2008), p. 5871–75
20. S. Lee, Y. Shin, S. Woo, K. Kim, H.-N. Lee, Review of Wireless Brain-Computer Interface Systems. In: R. Fazel-Rezai (ed.) Brain-Computer Interface Systems - Recent Progress and Future Prospects. InTech (2013). http://www.intechopen.com/books/brain-computer-interface-systems-recent-progress-and-future-prospects.
21. M Lopez-Gordo, D Morillo, F Pelayo, Dry EEG electrodes. Sensors **14**, 12847–12870 (2014)
22. IH Iversen, N Ghanayim, A Kübler, N Neumann, N Birbaumer, J Kaiser, A brain–computer interface tool to assess cognitive functions in completely paralyzed patients with amyotrophic lateral sclerosis. Clin. Neurophysiol. **119**, 2214–2223 (2008)
23. M van Gerven, O Jensen, Attention modulations of posterior alpha as a control signal for two-dimensional brain–computer interfaces. J. Neurosci. Methods. **179**, 78–84 (2009)
24. MA Lopez-Gordo, A Prieto, F Pelayo, C Morillas, Customized stimulation enhances performance of independent binary SSVEP-BCIs. Clin. Neurophysiol. **122**, 128–133 (2011)
25. J Thie, A Klistorner, SL Graham, Biomedical signal acquisition with streaming wireless communication for recording evoked potentials. Doc. Ophthalmol. **125**, 149–159 (2012)
26. NA Badcock, KA Preece, B de Wit, K Glenn, N Fieder, J Thie, G McArthur, Validation of the Emotiv EPOC EEG system for research quality auditory event-related potentials in children. PeerJ. **3**, e907 (2015)
27. M Caleffi, IF Akyildiz, L Paura, On the solution of the Steiner tree NP-hard problem via Physarum BioNetwork. IEEEACM Trans. Netw. **23**, 1092–1106 (2015)

28. GE Santagati, T Melodia, L Galluccio, S Palazzo, Medium access control and rate adaptation for ultrasonic intrabody sensor networks. IEEEACM Trans. Netw. **23**, 1121–1134 (2015)
29. JV Odom, M Bach, M Brigell, GE Holder, DL McCulloch, AP Tormene, Vaegan: ISCEV standard for clinical visual evoked potentials (2009 update). Doc. Ophthalmol. **120**, 111–119 (2010)
30. H Gevensleben, B Holl, B Albrecht, C Vogel, D Schlamp, O Kratz, P Studer, A Rothenberger, GH Moll, H Heinrich, Is neurofeedback an efficacious treatment for ADHD? A randomised controlled clinical trial. J. Child Psychol. Psychiatry. **50**, 780–789 (2009)
31. H Heinrich, H Gevensleben, U Strehl, Annotation: neurofeedback ? Train your brain to train behaviour. J. Child Psychol. Psychiatry. **48**, 3–16 (2007)
32. M Kouijzer, J Demoor, B Gerrits, M Congedo, H Vanschie, Neurofeedback improves executive functioning in children with autism spectrum disorders. Res. Autism Spectr. Disord. **3**, 145–162 (2009)
33. MEJ Kouijzer, JMH de Moor, BJL Gerrits, JK Buitelaar, HT van Schie, Long-term effects of neurofeedback treatment in autism. Res. Autism Spectr. Disord. **3**, 496–501 (2009)
34. ME Ayers, Neurofeedback for cerebral palsy. J. Neurother. **8**, 93–94 (2004)
35. A Bachers, Neurofeedback with cerebral palsy and mental retardation: a case report. J. Neurother. **8**, 95–96 (2004)
36. R Galambos, S Makeig, PJ Talmachoff, A 40-Hz auditory potential recorded from the human scalp. Proc. Natl. Acad. Sci. **78**, 2643–2647 (1981)
37. E Başar, B Rosen, C Başar-Eroglu, F Greitschus, The associations between 40 Hz-EEG and the middle latency response of the auditory evoked potential. Int. J. Neurosci. **33**, 103–117 (1987)
38. CD Bauch, DE Rose, SG Harner, Brainstem responses to tone pip and click stimuli. Ear Hear. **1**, 181–184 (1980)
39. W Szyfter, R Dauman, RC de Sauvage, 40 Hz middle latency responses to low frequency tone pips in normally hearing adults. J. Otolaryngol. **13**, 275–280 (1984)
40. Z-M Xu, E De Vel, B Vinck, PB van Cauwenberge, Choice of a tone-pip envelope for frequency-specific threshold evaluations by means of the middle-latency response: normally hearing subjects and slope of sensorineural hearing loss. Auris. Nasus. Larynx. **24**, 333–340 (1997)
41. C Borgmann, B Roß, R Draganova, C Pantev, Human auditory middle latency responses: influence of stimulus type and intensity. Hear. Res. **158**, 57–64 (2001)
42. DL Woods, C Alain, D Covarrubias, O Zaidel, Middle latency auditory evoked potentials to tones of different frequency. Hear. Res. **85**, 69–75 (1995)
43. R. Acharya, Navigation Signals. In: Understanding Satellite Navigation. pp. 83–153. Elsevier (2014). http://dx.doi.org/10.1016/B978-0-12-799949-4.00004-X.
44. A.L. Swindlehurst, B.D. Jeffs, Seco-Granados, G., Li, J.: Applications of Array Signal Processing. In: Academic Press Library in Signal Processing. pp. 859–953. Elsevier (2014). http://dx.doi.org/10.1016/B978-0-12-411597-2.00020-5.
45. BR Mahafza, *Radar Systems Analysis and Design Using Matlab* (Chapman & Hall/CRC, Boca Raton, 2000). https://www.google.es/url?sa=t&rct=j&q=&esrc=s&source=web&cd=1&cad=rja&uact=8&ved=0ahUKEwjz2LjnwP_KAhVB0BoKHc4mC6AQFggdMAA&url=http%3A%2F%2Fstaff.on.br%2Fpuxiu%2FMatLab_Pack%2FRadar%2520Systems%2520Analysis%2520and%2520Design%2520Using%2520MatLab%2520-%2520Mahafza%2520Bassem%2520R.pdf&usg=AFQjCNEJPGjDCyr8wuVJwjxa0GCAETMicA.
46. M. Parker, CDMA Wireless Communications. In: Digital Signal Processing 101. pp. 151–167. Elsevier (2010)
47. M. Ghogho, P. Ciblat, A. Swami, Synchronization. In: Academic Press Library in Signal Processing. pp. 9–94. Elsevier (2014). http://dx.doi.org/10.1016/B978-0-12-396500-4.00002-8.
48. MA Lopez-Gordo, DS Morillo, MAJ Van Gerven, Spreading codes enables the blind estimation of the hemodynamic response with short-events sequences. Int. J. Neural Syst **25**(1), 1411101801020006 (2014)
49. GT Buračas, GM Boynton, Efficient design of event-related fMRI experiments using M-sequences. NeuroImage. **16**, 801–813 (2002)
50. EE Sutter, Imaging visual function with the multifocal m-sequence technique. Vision Res. **41**, 1241–1255 (2001)
51. T Fawcett, An introduction to ROC analysis. Pattern Recognit. Lett. **27**, 861–874 (2006)
52. MA Lopez-Gordo, R Ron-Angevin, F Pelayo Valle, Auditory Brain-Computer Interfaces for Complete Locked-In Patients, in *Advances in Computational Intelligence*, ed. by J Cabestany, I Rojas, G Joya (Springer Berlin Heidelberg, Berlin, Heidelberg, 2011), pp. 378–385
53. H Jasper, Report of the committee on methods of clinical examination in electroencephalography. Electroencephalogr. Clin. Neurophysiol. **10**, 370–375 (1958)
54. SA Hillyard, RF Hink, VL Schwent, TW Picton, Electrical signs of selective attention in the human brain. Science. **182**, 177–180 (1973)
55. KA Yurgil, EJ Golob, Neural activity before and after conscious perception in dichotic listening. Neuropsychologia. **48**, 2952–2958 (2010)
56. MA Lopez-Gordo, F Pelayo, A Prieto, E Fernandez, An auditory brain-computer interface with accuracy prediction. Int. J. Neural Syst. **22**, 1–14 (2012)
57. MA Lopez-Gordo, E Fernandez, S Romero, F Pelayo, A Prieto, An auditory brain–computer interface evoked by natural speech. J. Neural Eng. **9**, 1–9 (2012)
58. C Guger, S Daban, E Sellers, C Holzner, G Krausz, R Carabalona, F Gramatica, G Edlinger, How many people are able to control a P300-based brain–computer interface (BCI)? Neurosci. Lett. **462**, 94–98 (2009)
59. IG Duncan, *Healthcare Risk Adjustment and Predictive Modeling* (ACTEX Publications, Winsted, Conn, 2011)
60. MA Lopez-Gordo, A Prieto, F Pelayo, C Morillas, Use of phase in brain–computer interfaces based on steady-state visual evoked potentials. Neural Process. Lett. **32**, 1–9 (2010)
61. M.A. Lopez-Gordo, F. Pelayo, A. Prieto, A high performance SSVEP-BCI without gazing. In: The 2010 International Joint Conference on Neural Networks (IJCNN) Barcelona, Spain (2010), pp. 193–197. http://ieeexplore.ieee.org/xpl/login.jsp?tp=&arnumber=5596325&url=http%3A%2F%2Fieeexplore.ieee.org%2Fxpls%2Fabs_all.jsp%3Farnumber%3D5596325